

# Surface roughness effects in granular matter: Influence on angle of repose and the absence of segregation

Nicholas A. Pohlman,<sup>1</sup> Benjamin L. Severson,<sup>2</sup> Julio M. Ottino,<sup>1,2</sup> and Richard M. Lueptow<sup>1,\*</sup>

<sup>1</sup>*Department of Mechanical Engineering, Northwestern University, Evanston, Illinois 60208, USA*

<sup>2</sup>*Department of Chemical and Biological Engineering, Northwestern University, Evanston, Illinois 60208, USA*

(Received 10 November 2005; published 16 March 2006)

We investigate the effect of nanoscale variations in the surface roughness of individual particles on macroscale granular flow characteristics. Experiments were conducted in circular rotating tumblers with smooth and rough 2 and 3 mm steel particles. The smooth beads had a rms surface roughness of approximately 30 to 60 nm; rough beads had a surface roughness of approximately 240 to 350 nm. The dynamic angle of repose for rough particles increased by  $10^\circ$  to  $25^\circ$  over that of smooth particles over a wide range of rotation speeds. Even though surface roughness affects the angle of repose, we were unable to detect any segregation of bidisperse mixtures of rough and smooth particles in the radial direction in two-dimensional (2D) tumblers. Furthermore, no axial banding segregation occurred in 3D tumblers, both cylindrical and spherical. For mixtures of smooth and rough particles, the angle of repose increased monotonically with increasing concentration of rough particles. Particle dynamics simulations verified that the dependence of the angle of repose on the concentration of rough particles can be directly related to the coefficient of friction of the particles. Simulations over a broad range of friction parameters failed to induce segregation solely from differences in the angle of repose. These results indicate that nanoscale surface roughness can affect the flowability and angle of repose of granular matter without driving demixing of the bulk granular material.

DOI: [10.1103/PhysRevE.73.031304](https://doi.org/10.1103/PhysRevE.73.031304)

PACS number(s): 45.70.Mg, 83.80.Fg

## I. INTRODUCTION

The nature of surface roughness and its influence on granular mixing and flow is a subject that has received little attention in granular flow studies. In most experiments, the surfaces of individual particles, typically spherical, in the flowing medium are implicitly assumed to be nominally “smooth.” However, this characteristic is rarely quantified. Due to the extraordinary number of contacting surfaces between discrete particles and because granular particles slide and roll with respect to one another when they flow, it is apparent that tribological effects can potentially play a major role in granular flow.

In general, it has been implicitly assumed that nanoscale surface effects are orders of magnitude less important than macroscopic properties such as particle size and density in granular flow. However, the coefficient of friction, a macroscale parameter, is often adjusted in discrete element modeling to produce significant changes in the granular flow characteristics [1–3]. Likewise, the experimentally determined angle of repose of a bulk material increases as the interaction friction is increased [4]. In fact, the conceptual relevance of the coefficient of friction to the angle of repose of a granular pile can be related to the simple problem of a block sliding down an inclined plane [5]. Of course, the macroscopic coefficient of friction merely reflects the multiple nanoscale surface interactions in granular flow.

Only a few researchers have attempted to quantify microscopic surface interactions between individual granular par-

ticles. For example, measurements indicate that surface properties influence the normal and tangential compliance of materials in both micro-slip and the gross sliding limit of friction [6]. More recent experiments coupling atomic force microscopy and annular shear cell tests focused on relating tribological properties to macroscale effects by introducing lubricants into a granular bulk of glass beads [7].

At a macroscopic scale, quasi-two-dimensional (2D) rotating drums, like that shown in Fig. 1, are often used to study the characteristics of flowing granular materials [8–11]. Typically, a cylinder is filled to 50% volume fraction with granular material and rotated about its axis causing the material to tumble down the angled free surface in a thin flowing layer. Upon reaching the end of the free surface, the material is trapped in near solid body rotation with the drum until it reaches the free surface again. Such tumblers provide a convenient means to measure the dynamic angle of repose. Moreover, quasi-2D and 3D rotating drums are often used to study granular segregation. Two initially well-mixed materials having different properties (such as size or density) tend to unmix leading to the classical radial segregation pattern in a quasi-two-dimensional tumbler [5,12–14] and bands of segregated material in a three-dimensional tumbler [15–17].

The focus of this paper is the relation between the friction due to the nanoscale surface roughness of a granular material and the macroscale granular flow properties. In particular, we consider the angle of repose for pure smooth or rough spherical particles as well as mixtures of these particles. As we shall demonstrate, surface roughness affects the dynamic angle of repose in rotating tumblers. And the angle of repose is widely believed to be a predictor of segregation. Is this, however, the case? To this end, we evaluate the tendency toward mixing or segregation of particles with differing sur-

\*Corresponding author. Electronic address: [r-lueptow@northwestern.edu](mailto:r-lueptow@northwestern.edu)

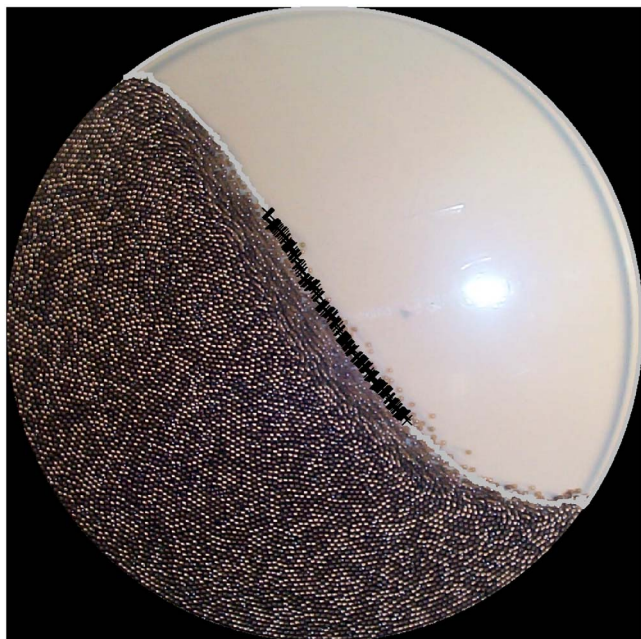


FIG. 1. (Color online) Single image of the quasi-2D rotating drum with 50% rough concentration of 2 mm particles at  $Fr = 6.07 \times 10^{-3}$ . A gray curve indicates the surface of the flowing layer from the ten ensemble averaged images and black  $\times$ 's show the middle 40% of the tumbler diameter.

face roughnesses in quasi-2D and 3D tumblers. In addition, we use particle dynamics simulations to further evaluate the influence of imposed friction characteristics on granular flows.

## II. EXPERIMENTAL APPROACH

### A. Chrome steel beads and their tribological characteristics

Spherical chrome steel beads (AISI 52100 Standard, Grade 1000, Fox Industries) having diameters of 2.37 mm (which we denote 2 mm) and 3.18 mm (3 mm) to within  $\pm 0.01$  mm were used in the experiments. Using smaller beads would have made the surface roughness measurements difficult and permitted electrostatic forces to interfere with the tumbler experiments described shortly. The new beads were shiny with a hard surface (62-65 on the Rockwell “C” scale). Rock polishing lapidary equipment (Lortone 3A Rotary Tumbler with super-coarse 46/70 silicon carbide grit) was used to roughen half of the beads. The rolling motion of the grit against the beads pitted the surface creating pock marks and eliminating the original shiny surface without altering the spherical shape or the diameter of the particles. The other half of the beads were used in their smooth, shiny state.

After cleaning the beads to remove the silicon carbide grit, the nanoscale surface profile of the beads was measured using a white light Phase-Shift interferometer (ADE Phase-Shift MicroXAM). The surface profile for a new smooth particle, shown in Fig. 2(a), is quite smooth with only a few short asperities. The surface profile of a rough particle, shown in Fig. 2(b), has many more asperities, nearly all hav-

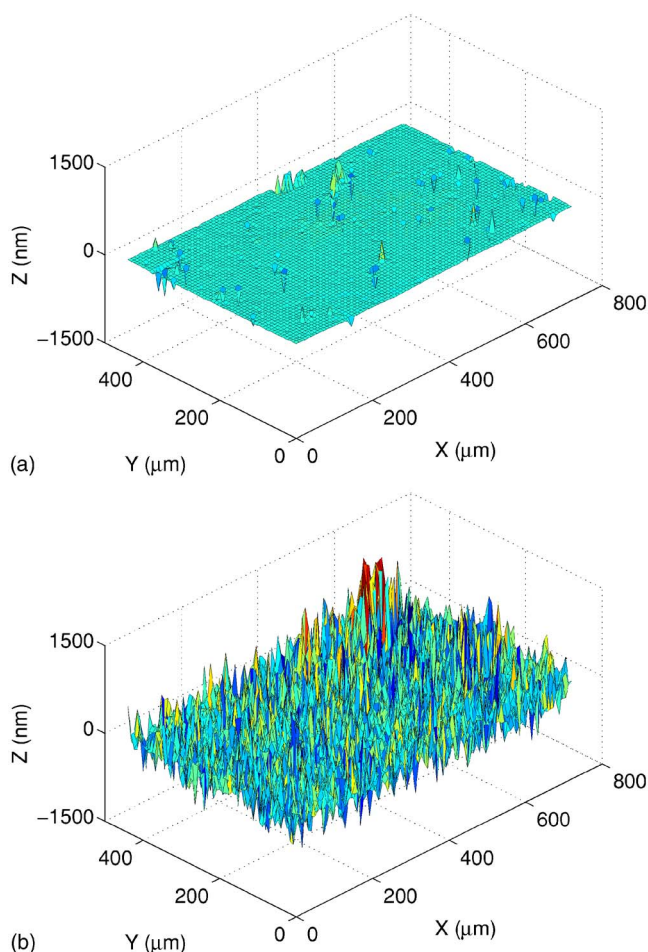


FIG. 2. (Color online) Typical surface profile for 2 mm particles for (a) new material and (b) after roughening.

ing much larger magnitudes than those of the smooth bead. The surface roughness  $R_q$  of the material is defined as the standard deviation of the measured height. Only a small portion of the bead surface ( $\approx 800 \mu\text{m} \times 600 \mu\text{m}$ ) can be measured at one time, so multiple measurements on a single bead were used to verify that the measured surface roughness was equivalent over the entire surface. The surfaces of at least 35 particles per lot of material were measured with the averaged surface roughness results given in Table I for a typical lot of the new and roughened beads. Even with the extraordinary hardness of the base material, there was some degradation in the surface roughness after the beads were tumbled in a rotating drum, as is evident in the change in the roughness from the “Pre-test” values to the “Post-test” values for the

TABLE I. Typical surface roughness ( $R_q$ ) of beads used in experimentation (all roughness values are in nanometers).

	Ball size			
	2 mm		3 mm	
	New	Roughened	New	Roughened
Pre-test	$26 \pm 9$	$235 \pm 29$	$59 \pm 11$	$244 \pm 31$
Post-test	$31 \pm 10$	$160 \pm 34$	$57 \pm 13$	$174 \pm 30$

TABLE II. Mean of the coefficient of friction for six tests of 3 mm rough and smooth particles on a machine ground surface and a polished surface. (Surface roughness of the beads is different from Table I due to different lots of material.)

Surface Condition	Normal Force (mN)	Coefficient of Friction ( $\mu$ )	Friction Intensity
 $R_q = 235$ nm	49	$0.22 \pm 0.03$	
	147	$0.19 \pm 0.03$	
	245	$0.15 \pm 0.01$	
 $R_q = 29$ nm	49	$0.26 \pm 0.05$	
	147	$0.23 \pm 0.03$	
	245	$0.28 \pm 0.07$	
 $R_q = 56$ nm	49	$0.11 \pm 0.01$	
	147	$0.12 \pm 0.01$	
	245	$0.11 \pm 0.01$	
 $R_q = 29$ nm	49	$0.27 \pm 0.02$	
	147	$0.44 \pm 0.03$	
	245	$0.48 \pm 0.03$	

roughened particles. Most likely, plastic deformation occurred due to the asperity interactions of the rough surfaces when particles collided. The decay of the surface properties was limited by keeping the total number of revolutions of the tumbler to less than 400.

The macroscale friction characteristics of the granular particles were measured in three ways: a scratch test, acceleration of sliding particles down an angled slope, and the critical angle to cause particles at rest to start sliding.

A standard tribological scratch test determines the dynamic coefficient of friction via the ratio of drag force to the applied normal force. A CETR Tribometer held a single 3 mm bead at a constant normal force on a flat disk and measured the transverse force while the bead was slid without rolling at a constant velocity across the disk. Due to their small size, 2 mm beads could not be tested in this apparatus. Table II reports the mean and standard deviation of at least six measurements of the coefficient of friction. The schematics in the "Surface Condition" column show the surface roughnesses of the spherical particles and the flat surfaces (the relative surface heights are not to scale). The shading in the "Friction Intensity" column provides a visual indication of the relative magnitudes of the coefficient of friction with black showing  $\mu=0.5$  and white indicating a frictionless sliding contact. Rough particles tested on a machine ground flat steel surface ( $R_q=544$  nm) had a higher coefficient of friction than smooth particles on the same surface, as expected, but the coefficient of friction depended on the normal force. When the particles were tested on a flat steel surface polished to a mirror finish ( $R_q=29$  nm), the coefficient of friction was higher for the smooth particles than for the rough particles, especially at higher normal forces.

Although these results seem counterintuitive, they are consistent with the theory of tribological surface interaction. Macroscale friction is a function of the normal force between two surfaces, not the area of contact. However, when the contact area is significantly reduced, such as in near single point contact between a sphere and a flat surface, the nature of the contact becomes critically important. The rough beads probably have a higher coefficient of friction on the machine ground flat surface than the smooth beads because a greater number of asperities are in contact between the two surfaces, requiring a greater tangential shear necessary for relative motion. The reduction in the coefficient of friction for the rough particles on the same surface with an increasing normal force is likely a result of plastically deforming the asperities. The smooth bead on the machine ground flat surface reduces total asperity contact, and the corresponding coefficient of friction is less. The smooth particle on a polished flat surface results in a remarkable increase in the coefficient of friction compared to the cases where at least one of the surfaces is rough. This is likely due to the increased stiction between the two surfaces due to the lack of asperity interaction on the micro-scale level.

The minimum normal force available in the CETR Tribometer corresponds to weight of more than 37 particles (the weight of a single bead is 1.3 mN), which is much larger than the total depth of the flowing layer in a typical tumbler experiment, usually 7–10 particles. Therefore, two other methods having contact forces generated by the mass of individual particles were used to characterize the coefficient of friction. In the first case, the dynamic coefficient of friction was measured based on the acceleration of sliding particles on a sloped flat surface. In order to prevent rolling and maintain a sliding contact, a tripod of three 3 mm particles was bonded together with an adhesive. The tripod was released on a flat surface tilted at a known angle  $\theta$  with respect to the horizontal, and its motion was recorded with a digital video camera. Assuming a constant acceleration, the coefficient of friction was calculated as  $\mu = \tan(\theta) - 2A/(g \cos \theta)$ , where  $A$  is the coefficient of the squared term in a parabolic fit to the position of the tripod with respect to time. The smooth and rough plates were made of AISI 52100 chrome steel, the same alloy as the particles, so as to mimic particle-to-particle interactions in a granular flow. Acrylic was also used as a flat surface to characterize contacts between particles and the material of the drum walls. Results averaged over 30 or more trials of every combination of surface-bead contacts are reported in Table III (the transparent acrylic surface is schematically represented by a dashed line).

The results match the intuition that rough particles have a higher coefficient of friction. However, it is interesting to note the factor of 2 increase in the coefficient of friction as the chrome steel flat surface changes from the rough machine ground to the smooth mirror finish. Again, it appears that the lack of asperities on the mirror polished surface results in a greater number of contacts between the surfaces causing an increase in the measured coefficient of friction.

Finally, the static friction was characterized by measuring the critical angle of a flat surface that induces motion of a particle tripod set. The experiment was conducted by placing a tripod on a horizontal flat surface which was then tilted

TABLE III. Average and standard deviation of the coefficient of friction from at least 30 runs of tripods sliding down a flat surface. The surface roughness is the average over the three particles of the tripod.

Surface Condition	Coefficient of Friction ( $\mu$ )	Friction Intensity
 $R_q = 235$ nm $R_q = 304$ nm	$0.16 \pm 0.02$	
 $R_q = 235$ nm $R_q = 23$ nm	$0.35 \pm 0.07$	
 $R_q = 235$ nm $R_q = \text{N/A}$	$0.44 \pm 0.02$	
 $R_q = 56$ nm $R_q = 304$ nm	$0.14 \pm 0.01$	
 $R_q = 56$ nm $R_q = 23$ nm	$0.25 \pm 0.02$	
 $R_q = 56$ nm $R_q = \text{N/A}$	$0.35 \pm 0.07$	

very slowly ( $1.5^\circ/\text{sec}$ ) until the tripod began sliding. The average angle that initiated the sliding motion averaged over at least 60 trials is reported in Table IV. The schematics in each column represent the relative surface roughness between the particles and the flat surface, which are oriented at the angle that sliding occurred for that particle and flat surface combination. In this case, the 2 mm particles were also evaluated. The key result is that the critical sliding angle increases for all cases when the surface roughness of the particles changes from smooth to rough. The large standard deviation is indicative of the difficulty in obtaining repeatable measurements.

All three methods of characterizing friction suggest that increased surface roughness of particles generally causes a corresponding increase in the observed friction, although exceptions occur depending upon the roughness of the flat surface. It is clear that quantifying and obtaining consistent values of the macroscale friction based on the surface roughness of contacting surfaces for individual particles is quite difficult.

TABLE IV. Critical angle to initiate the sliding of a tripod of particles. At least 60 trials were conducted for each particle size and surface roughness combination. The surface roughness is the average over the three particles of the tripod.

Flat Surface	Mirror Polish $R_q = 23$ nm		Machine Ground $R_q = 304$ nm		Acrylic Transparent	
Particle Size	2 mm					
Particle $R_q$ (nm)	34.1 	250.8 	55.5 	168.5 	33.6 	277.8 
Sliding Angle	$11.4^\circ \pm 2.0^\circ$	$21.6^\circ \pm 7.5^\circ$	$12.8^\circ \pm 2.0^\circ$	$16.8^\circ \pm 4.4^\circ$	$28.2^\circ \pm 8.1^\circ$	$33.8^\circ \pm 6.8^\circ$
Particle Size	3 mm					
Particle $R_q$ (nm)	59.3 	284.2 	43.4 	246.0 	37.9 	343.8 
Sliding Angle	$16.3^\circ \pm 3.3^\circ$	$23.4^\circ \pm 6.3^\circ$	$12.4^\circ \pm 2.0^\circ$	$15.2^\circ \pm 3.5^\circ$	$27.2^\circ \pm 6.9^\circ$	$29.9^\circ \pm 4.5^\circ$

**B. Rotating tumbler**

The collective effect of the surface roughness of many particles on the granular flow was measured using a quasi-2D tumbler with a diameter of  $2R=28$  cm and a thickness of  $2.8d$ , where  $d$  is the particle diameter (the thickness was adjusted according to the particle size). These dimensions were chosen to provide a large drum diameter to particle diameter ratio,  $2R/d:118$  and  $88$  for  $d=2$  and  $3$  mm, respectively. The thickness of the quasi-2D tumbler was necessarily small to reduce the quantity of particles that were used. This was particularly important due to the cost of the particles, which could only be used for a limited time because the surface properties changed with use, as indicated in Table I. The front and back plates of the tumbler were 6.4 mm thick, clear, static-dissipative acrylic allowing visualization of the free-flowing surface and measurement of the angle of repose. The surfaces of the acrylic were electrically grounded to minimize electrostatic charge buildup in the tumbler.

The dynamics of the flow in a rotating drum are governed by the Froude number [5],  $Fr=R\omega^2/g$ , where  $\omega$  is the rotational speed and  $g$  is the gravitational acceleration, which represents the ratio of centrifugal to gravitational forces acting on the particles in the drum. By changing the rotational speed, the Froude number was varied from  $10^{-5}$ , just fast enough so that the flow was continuous (not avalanching), to  $1.5 \times 10^{-2}$ , which was well into the cataracting regime of flow. The tumbler rotation was controlled with a brushless stepper motor and a microstep driver with input control to the driver via a computer controlled square wave generator. In all cases, the fill level of the drum was 50%.

To measure the dynamic angle of repose  $\beta_d$ , ten high resolution digital images of the rotating tumbler were obtained at each Froude number. The drum was stopped while the images were downloaded in order to reduce wear of the particle surfaces. The motor was then accelerated from rest to the next Froude number. The intensity from ten digital images for each Froude number was ensemble averaged and, after eliminating the extraneous background via image processing, the surface profile of the flowing granular material was located with an edge-find function, producing results like that shown in Fig. 1. Only the central 40% of the edge, evident as the dark  $\times$ 's near the surface, was used for the linear fit to determine the dynamic angle of repose, thus avoiding the curved free surface near the periphery of the tumbler.

### III. EXPERIMENTAL RESULTS

#### A. Monodisperse angle of repose

To begin, we report the dynamic angle of repose,  $\beta_d$ , of monodisperse smooth and monodisperse rough particles. For the smooth 2 mm particles, the angle of repose was  $26.2^\circ$  at  $Fr=2.0 \times 10^{-4}$ . The smooth 3 mm particles at the same rotation rate had a lower dynamic angle of repose of  $23.4^\circ$ . The higher angle of repose with decreased particle size is consistent with previous results [8]. When the contents of the drum were changed to rough 2 mm and 3 mm particles, the angles of repose increased to  $43.4^\circ$  and  $31.1^\circ$ , respectively, for the same Froude number, clearly indicating that the angle of repose of a bulk material is directly related to the surface roughness of the individual particles. Most likely, interlocking asperities result in greater sliding and rolling friction between rough particles than for particles having smooth surfaces so that rough particles pile up at a higher angle before gravity can overcome the interparticle friction.

After the experiments, the surface roughness of the particles was measured to determine the wear due to tumbling, with the results given for the monodisperse rough and smooth systems in Table I. The surface roughness of the smooth particles was within a standard deviation of the pre-tumbled particles. The “smoothing” of rough particles was much greater with a decrease between 24% and 34% from the initial surface roughness. The difference in wear between rough and smooth particles can be attributed to greater plastic deformation of the taller asperities of the roughened particles due to collisional impact.

#### B. Do different angles of repose cause segregation?

One of the interesting aspects of granular flow is the segregation of polydisperse material. For instance, in a quasi-2D tumbler, radial segregation occurs with small or dense particles gathering at the center of the fixed bed and the remaining material near the periphery [5]. The radial segregation can be explained in terms of percolation, where the smaller particles fall through the voids in the lattice of larger particles, or buoyancy, where more dense particles sink to lower levels in the flowing layer [13,18].

A theoretical approach to predicting segregation is based on the angle of repose of each member of a bidisperse system, regardless of the particle size or density. For instance, a cellular automata model predicts that radial segregation can occur in rotating drums when two distinct particles fall at different angles of repose due to the individual particle friction [19].

Given these models for radial segregation based on particles with different angles of repose, and that pure rough and smooth beads exhibit different angles of repose, we attempted to find a situation in which the rough and smooth particles segregated. However, no radial segregation was observed for the bidisperse (smooth and rough) mixtures in the quasi-2D tumbler for Froude numbers ranging from  $3.9 \times 10^{-7}$  to  $1.5 \times 10^{-3}$ , an example of which is shown in Fig. 1. Even when the materials started in an unmixed state (each particle type filling a sector of the drum), the two species mixed thoroughly. In addition, there was no preferential

neighboring of rough or smooth particles based on an analysis of the connectivity of smooth-to-smooth or rough-to-rough particles after a few rotations of the system. Thus, it appears that differences in surface roughness characteristics alone cannot cause radial segregation, even though the angles of repose of the two species differ substantially.

In three-dimensional situations, either long cylinders or spherical containers, bands of segregated material spontaneously form and then coarsen due to differences in particle size [15–17,20,21]. The differing angles of repose for the two components of a bidisperse mixture is key in the explanation of how bands are produced in three-dimensional experiments [22,23]. This mechanism is predicated upon a radial core preceding the formation of enriched bands of particles that are observed in axial segregation.

We also performed experiments in 3D (spherical) and 2D+1 (cylindrical) granular systems to explore the potential for banding of rough and smooth particles given their differing angles of repose. In a 3D spherical container with a diameter of 35 particles, the rotation of a mixture of rough and smooth particles at 50% volume fraction over 10 h at a Froude number of  $6 \times 10^{-3}$  to generate a continuous, flat flowing layer resulted in no banding. A similar test in a half-filled cylinder with a 76.2 mm diameter (32 particles) and 185 mm length rotated at  $Fr=6.1 \times 10^{-3}$  also did not produce segregated bands over a test run of 72 h. In fact, starting with one-half of the length of the tube half-filled with rough particles and the other half with smooth particles only produced diffusion of the rough and smooth particles rather than maintaining axial segregation. There was a clear difference in the angle of repose between the two different materials. However, this did not prevent the mixing of the two particle types. Thus, while the surface roughness can change the angle of repose of the bulk material, this characteristic alone does not appear to be a sufficient condition for segregation, at least for the conditions used in this study. This further suggests that radial segregation as a result of percolation or buoyancy is a necessary precursor to axial segregation and subsequent axial banding.

#### C. Angle of repose of bidisperse mixtures

Although the difference in the angles of repose of the smooth and rough beads does not cause segregation, it may alter the nature of the granular flow for bidisperse mixtures of smooth and rough beads. Hence, the dynamic angle of repose was measured as a function of the Froude number for a variety of mixtures of the smooth and rough 2 and 3 mm beads at concentrations ranging from 0% rough to 100% rough as shown in Fig. 3. To assure that the measured angle of repose was related to the Froude number and not a result of the changes in the surface roughness of the beads due to wear, the measurements were conducted by increasing the rotational speed to obtain data for every other Froude number in Fig. 3. Then, the remaining data were obtained by decreasing the rotational speed. In addition, multiple data points at the same Froude number identify rotational speeds that were retested in order to verify the repeatability of the measurements. Although there was a measurable decrease in

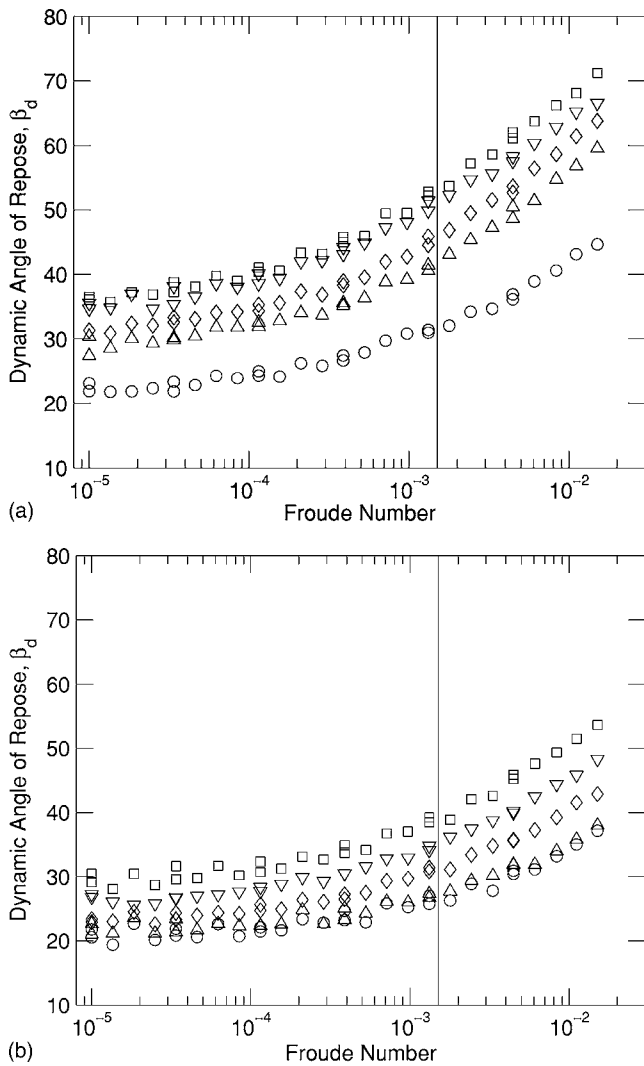


FIG. 3. Angle of repose as a function of the Froude number for (a) 2 mm and (b) 3 mm beads for different concentrations of rough particles;  $\circ$ =0% rough concentration,  $\triangle$ =25% rough,  $\diamond$ =50% rough,  $\nabla$ =75% rough, and  $\square$ =100% rough.

the rough particle surface roughness during an experiment, as indicated in Table I, the angle of repose remained only a function of the concentration of rough particles and the Froude number.

The results in Fig. 3 show that the angle of repose increases with increasing Froude number, consistent with previous results [8], regardless of particle size or rough particle concentration. Above approximately  $Fr=1.5 \times 10^{-3}$  (marked by the vertical lines in Fig. 3), the free surface becomes curved indicating a transition to the cataracting regime of flow. More importantly, the angle of repose increases as the concentration of rough particles increases, which is shown more clearly in Fig. 4. At low Froude numbers, the angle of repose for the 2 mm beads increases by about  $15^\circ$  as the concentration changes from purely smooth to purely rough particles. At higher Froude numbers, the change in the angle of repose as the concentration of rough beads increases is even larger, greater than  $25^\circ$  at the highest speed. The changes in the angle of repose from one concentration to

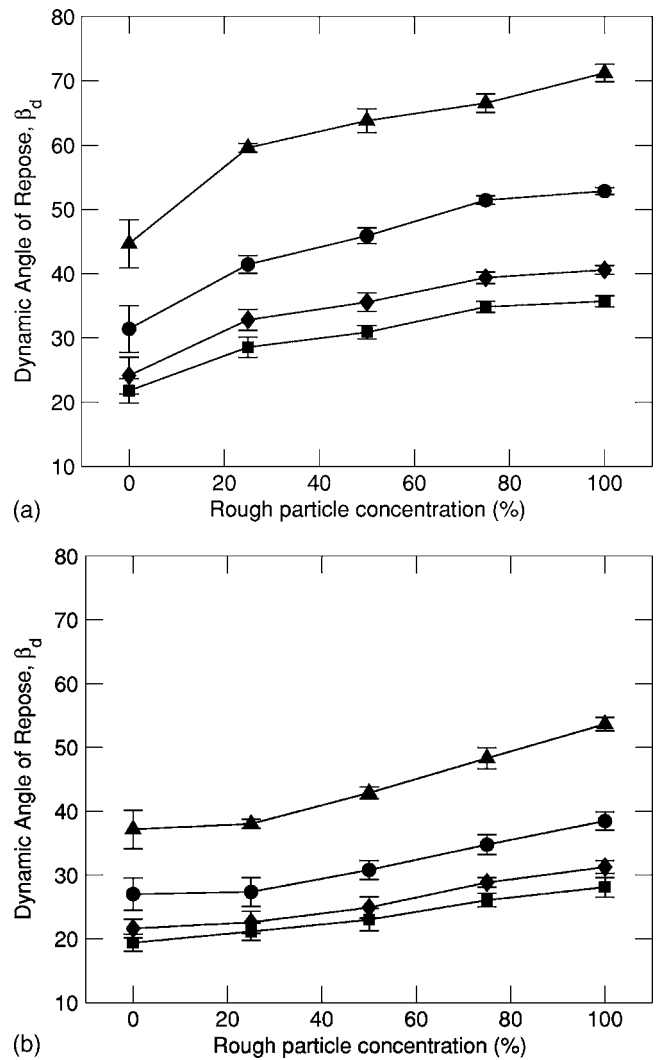


FIG. 4. Angle of repose as a function of concentration of rough particles for (a) 2 mm and (b) 3 mm beads for different Froude numbers;  $\blacksquare$   $Fr=1.4 \times 10^{-5}$ ,  $\blacklozenge$   $Fr=1.6 \times 10^{-4}$ ,  $\bullet$   $Fr=1.3 \times 10^{-3}$ , and  $\blacktriangle$   $Fr=1.5 \times 10^{-2}$ . Error bars represent the standard deviation for the angle of repose measurement for ten individual images.

another at the same Froude number are somewhat less for the 3 mm beads, particularly when the rough particle concentration changes from 0% to 25%. The difference may be a consequence of the surface roughness of the smooth beads. Table I indicates that the smooth 2 mm particles had a smaller surface roughness than the smooth 3 mm particles. It is possible that small concentrations of rough particles with very smooth particles may have more influence on the angle of repose than when the smooth particles are not quite as highly polished. It is also evident that the angle of repose is greater in all cases for the smaller beads than for the larger beads, consistent with previous results [8]. Fig. 4 also indicates the variability of the angle of repose measurement when individual images are used rather than ensemble averaging the raw image intensity. The largest standard deviation occurs for the 0% rough concentration. The shiny appearance of the smooth particles makes it difficult for the edge-find function to differentiate between the free surface of particles

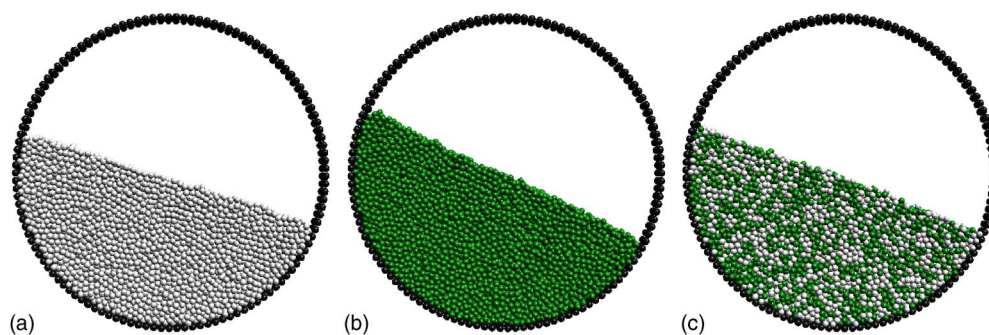


FIG. 5. (Color online) Single instances of the PD simulations for the following friction conditions: (a)  $\mu=0.1$  for all particles (0% rough concentration); (b)  $\mu=0.5$  for all particles (100% rough concentration); (c) 50% rough particle concentration where  $\mu=0.1$  between light particles,  $\mu=0.5$  between dark particles, and  $\mu=0.3$  for mixed contacts.

and the background in an individual image. Otherwise, the standard deviation is independent of the Froude number or concentration of rough particles.

Besides surface roughness, other microscopic forces can influence the angle of repose for granular flow. For instance, electrostatic attraction forces between the walls and the particles can increase the angle of repose. Furthermore, particle impacts induce magnetic properties in the steel beads that can cause small attraction forces between particles. As a precaution, prior to all experimental runs the beads were passed through an oscillating magnetic field to minimize the induced magnetic attraction between particles. Surprisingly, the thickness of the acrylic end plates also affected the angle of repose. Increasing the thickness of the acrylic end plates from 6.4 to 9.5 mm caused an increase of  $3-4^\circ$  in the angle of repose for otherwise similar conditions. This may be a result of a slight decrease in the axial drum length as the thicker cover plate flexed outward less due to the axial pressure of the fixed bed of steel beads. Further tests verified that increasing  $t/d$  from 2.8 particles to 5 and 7 resulted in a decrease in the measured angle of the repose, consistent with previous results in a granular heap flow [24–26] and rotating tumbler flow [27]. Nevertheless, the trend of the increasing angle of repose with increasing concentration of rough particles occurred regardless of the value of  $t/d$ . Thus, the surface roughness is the primary factor causing a change in the angle of repose of granular flow for the results shown in Figs. 3 and 4.

#### IV. SIMULATION OF PARTICLES WITH VARYING FRICTION

Particle dynamics (PD) simulations have been shown to accurately capture many aspects of granular materials in a rotating tumbler [10,28], including segregation of bidisperse particles [29–34]. Here PD simulations have the advantage over experiments in that the method provides precise control over the factors influencing the particle contact allowing the isolation of the causes of flow behavior. In this way, the difficulty in measuring the coefficient of friction between rough-smooth surfaces and rough-smooth particles can be circumvented by simply assigning different friction characteristics to two classes of particles in the simulations.

The simulation consisted of solving the fundamental equations of motion for each particle given the normal and tangential forces,  $f_n$  and  $f_t$ , being applied by other particles in contact [29]. The parameters of the particle interaction were the spring stiffness in the normal and tangential directions,  $k_n$  and  $k_t$ , the damping of particle velocity after contact,  $k_d$ , and the coefficient of friction between sliding surfaces,  $\mu$ . The normal forces were modeled via the Hertzian overlap [35], while the tangential force was computed as the minimum between (1) the product of the normal force and the coefficient of friction ( $f_n\mu$ ) or (2) the restoring force from the tangential spring and lateral displacement ( $k_t\delta$ ). The free moving granular particles were constrained in a circular boundary of particles that held a fixed radial position but rotated as an entire ring at a specified rotation rate. The simulated tumbler had a diameter of 40 particles and a rotation rate of 1.05 revolutions per minute producing a Froude number of  $4.94 \times 10^{-5}$ . Periodic boundary conditions were assumed in the axial direction of the simulated tumbler. The particle parameters were based on the typical material properties of the chrome steel beads used in the experiments ( $k_n=4.44 \times 10^9$  N/m<sup>3/2</sup>,  $k_t=7.23 \times 10^5$  N/m, and  $k_d=380$  Ns/m<sup>3/2</sup>) with a time step of  $\Delta t=2.76 \times 10^{-7}$  s.

A sensitivity analysis was performed to determine the most important parameters that influence the angle of repose in the simulations. The stiffnesses, coefficient of friction, and damping were varied by an order of magnitude, but the angle of repose was only influenced by changes in the coefficient of friction. Therefore, investigations were limited to low and high friction between particles. Single snapshots of the simulation results with low friction particles ( $\mu=0.1$ ) and high friction particles ( $\mu=0.5$ ) are shown in Figs. 5(a) and 5(b), respectively. After achieving steady flow, the angle of repose of particles at the free surface was averaged over 250 simulation configurations distributed over more than one-quarter revolution of the drum so that more than half of the particles passed through the flowing layer. For the condition of  $\mu=0.1$ , the angle of repose was  $16.9 \pm 0.9^\circ$ . It increased to  $24.7 \pm 1.1^\circ$  when the coefficient of friction was set at  $\mu=0.5$ . While the magnitudes of the angle of repose do not match the experimental results, the increased interparticle friction causing an increase in the angle of repose is qualitatively consistent. The likely reason for the differences between experimental and simulation results is the limited size

of the simulated tumbler due to the computation being constrained to a reasonable number of particles (4000).

To model mixtures of smooth and rough particles, bidisperse mixtures of low friction and high friction particles were simulated. One of the difficulties is determining the value of the coefficient of friction that should be used for interactions between the low friction and high friction particles in simulating the mixture. In this case, such interactions were assumed to have a coefficient of friction of  $\mu = 0.3$ , the average of the low and high friction particles. The resulting angle of repose was  $19.9 \pm 0.9^\circ$  for a 50% rough concentration, shown in Fig. 5(c). Simulations at other concentrations of rough particles resulted in a linear relationship between the concentration of high friction particles and the angle of repose. Thus, the particle dynamics simulations confirmed that the angle of repose changes by varying only the coefficient of friction.

Finally, a benefit of the particle dynamics simulation is the knowledge of every particle position. A statistical analysis verified that the number of contacts between low-low, high-high, and mixed friction particles matched the expectation for a random distribution of particle contacts. This also matches the experimental observation of complete mixing of particles having different frictional properties with no tendency toward segregation.

## V. CONCLUSIONS

It is clear that nanoscale surface roughness of a granular material can affect the macroscale behavior. The dynamic angle of repose is greater for rough particles than for smooth particles over a wide range of Froude numbers. Furthermore, as the concentration of rough particles increases, a corresponding increase in angle of repose occurs, regardless of the

Froude number. However, it is quite difficult experimentally to wholly capture the effect of the surface roughness solely in terms of the coefficient of friction. The contact area between particles is so small that the interlocking of asperities and stiction can play a major role. Nevertheless, particle dynamics simulations verified that increasing the coefficient of friction between particles alone increases the angle of repose of the bulk material just as increasing the fraction of rough particles does.

Even though the angles of repose of the rough and smooth particles differed substantially, this did not result in either radial segregation in quasi-two-dimensional tumblers or banding in three-dimensional tumblers for bidisperse mixtures. The absence of segregation both experimentally and computationally suggests that the segregation mechanisms based solely on surface roughness or the angle of repose need to be reconsidered. A variation in the angle of repose may be necessary for segregation but is clearly not sufficient. While both properties of surface roughness and angle of repose may play a role in the flowability of granular material, they do not by themselves appear to cause segregation.

## ACKNOWLEDGMENTS

This work was funded in part by the Office of Basic Energy Sciences of the Department of Energy (Grant No. DE-FG02-95ER14534), and by the National Science Foundation IGERT Programs “Dynamics of Complex Systems in Science and Engineering” (Grant No. DGE-9987577) and “Virtual Tribology” (Grant No. DGE-0114429). Also, thanks to Qian Wang for providing access to the ADE Phase-Shift MicroXAM and CETR Tribometer to characterize the surface properties of the granular material. Thanks to Paul Umbanhowar for several useful discussions.

- 
- [1] A. Karolyi, J. Kertesz, S. Havlin, H. A. Makse, and H. E. Stanley, *Europhys. Lett.* **44**, 386 (1998).
  - [2] D. I. Goldman, M. D. Shattuck, S. J. Moon, J. B. Swift, and H. L. Swinney, *Phys. Rev. Lett.* **90**, 104302 (2003).
  - [3] Y. C. Zhou, B. H. Xu, A. B. Yu, and P. Zulli, *Phys. Rev. E* **64**, 021301 (2001).
  - [4] Y. C. Zhou, B. H. Xu, A. B. Yu, and P. Zulli, *Powder Technol.* **125**, 45 (2002).
  - [5] G. H. Ristow, *Pattern Formation in Granular Materials* (Springer, Berlin, 2000), Vol. 164.
  - [6] M. Mullier, U. Tuzun, and O. R. Walton, *Powder Technol.* **65**, 61 (1991).
  - [7] R. G. Cain, N. W. Page, and S. Biggs, *Phys. Rev. E* **62**, 8369 (2000).
  - [8] A. V. Orpe and D. V. Khakhar, *Phys. Rev. E* **64**, 031302 (2001).
  - [9] K. M. Hill, G. Gioia, and V. V. Tota, *Phys. Rev. Lett.* **91**, 064302 (2003).
  - [10] C. M. Dury, G. H. Ristow, J. L. Moss, and M. Nakagawa, *Phys. Rev. E* **57**, 4491 (1998).
  - [11] S. N. Dorogovtsev and J. F. Mindes, *Eur. Phys. J. E* **5**, 441 (2001).
  - [12] N. Thomas, *Phys. Rev. E* **62**, 961 (2000).
  - [13] N. Jain, J. M. Ottino, and R. M. Lueptow, *Granular Matter* **7**, 69 (2005).
  - [14] G. Félix and N. Thomas, *Phys. Rev. E* **70**, 051307 (2004).
  - [15] Y. Oyama, *Bull. Inst. Phys. Chem. Res.* **18**, 600 (1939).
  - [16] B. Roseman and M. B. Donald, *Int. Chem. Eng.* **7**, 823 (1962).
  - [17] S. J. Fiedor and J. M. Ottino, *Phys. Rev. Lett.* **91**, 244301 (2003).
  - [18] S. B. Savage and C. K. Lun, *J. Fluid Mech.* **189**, 311 (1988).
  - [19] P. Y. Lai, L.-C. Jia, and C. K. Chan, *Phys. Rev. Lett.* **79**, 4994 (1997).
  - [20] Z. S. Khan and S. W. Morris, *Phys. Rev. Lett.* **94**, 048002 (2004).
  - [21] J. F. Gilchrist and J. M. Ottino, *Phys. Rev. E* **68**, 061303 (2003).
  - [22] K. M. Hill and J. Kakalios, *Phys. Rev. E* **52**, 4393 (1995).
  - [23] S. Das Gupta, D. V. Khakhar, and S. K. Bhatia, *Chem. Eng. Sci.* **46**, 1513 (1991).
  - [24] N. Taberlet, P. Richard, A. Valance, W. Losert, J. M. Pasini, J. T. Jenkins, and R. Delannay, *Phys. Rev. Lett.* **91**, 264301 (2003).

- (2003).
- [25] N. Taberlet, P. Richard, E. Henry, and R. Delannay, *Europhys. Lett.* **68**, 515 (2004).
- [26] S. B. Ogalea, R. N. Bathea, R. J. Choudharya, S. N. Kalea, A. S. Ogalea, A. G. Banpurkarb, and A. V. Limaye, *Physica A* **354**, 49 (2005).
- [27] N. A. Pohlman, J. M. Ottino, and R. M. Lueptow (unpublished).
- [28] R. Y. Yang, R. P. Zou, and A. B. Yu, *Powder Technol.* **130**, 138 (2003).
- [29] J. J. McCarthy, T. Shinbrot, G. Metcalfe, J. E. Wolf, and J. M. Ottino, *AIChE J.* **42**, 3351 (1996).
- [30] C. M. Dury and G. H. Ristow, *J. Phys. I* **7**, 737 (1997).
- [31] J. J. McCarthy and J. M. Ottino, *Powder Technol.* **97**, 91 (1998).
- [32] C. M. Dury and G. H. Ristow, *Phys. Fluids* **11**, 1387 (1999).
- [33] J. J. McCarthy, D. V. Khakhar, and J. M. Ottino, *Powder Technol.* **109**, 72 (2000).
- [34] D. C. Rapaport, *Phys. Rev. E* **65**, 061306 (2002).
- [35] J. Schafer, S. Dippel, and D. E. Wolf, *J. Phys. I* **6**, 5 (1996).